

Highly reflective distributed Bragg reflectors using a deeply etched semiconductor/air grating for InGaN/GaN laser diodes

Tadashi Saitoh,^{a)} Masami Kumagai, Hailong Wang,^{b)} Takehiko Tawara, Toshio Nishida, Testuya Akasaka, and Naoki Kobayashi
 NTT Basic Research Laboratories, NTT Corporation, 3-1, Morinosato-Wakamiya, Atsugi, Kanagawa 243-0198, Japan

(Received 4 April 2003; accepted 28 April 2003)

High reflectivity is achieved by deeply etched InGaN/GaN distributed Bragg reflector (DBR) mirrors with tilted sidewalls, which are appropriately designed by using the finite-difference time-domain method. The predicted optimal structure is different from the simple design consisting of a $\lambda/(4n)$ semiconductor and $\lambda/4$ air. If the sidewall of the grating is tilted by 4° , the reflectivity of the DBR mirrors decreases to less than 40%. However, any degradation in the reflectivity of a perfectly vertical sidewall can be suppressed to just a few percent even with a sidewall tilt of 4° , if the DBR structure is properly designed. We fabricated InGaN/GaN multiple-quantum well lasers based on the optimal design. The devices operate as lasers with optical pumping at a lower threshold than devices without DBR mirrors. The DBR mirror reflectivity is characterized by the relation between the threshold pump intensity and the inverse of the cavity length, resulting in a high reflectivity of 62%. © 2003 American Institute of Physics. [DOI: 10.1063/1.1586992]

InGaN/GaN lasers¹ are attracting a great deal of attention as blue/violet light sources for the next generation of storage systems such as the Blu-ray Disk.² However, the operating current of InGaN/GaN lasers is much higher than that of conventional GaAs/AlGaAs or GaInAsP/InP lasers. One reason for this high threshold is their low facet reflectivity of only about 18%, which results from the low refractive indices of GaN-based materials of about 2.5. The lifetime of InGaN/GaN lasers is strongly dependent on the operating current, which must therefore be reduced. To achieve this, multiple dielectric films are usually coated on the facets, but this adds extra processing steps to laser fabrication. A promising alternative structure for laser mirrors is a deeply etched distributed Bragg reflector (DBR).³⁻⁹ Marinelli *et al.*¹⁰ have demonstrated deeply etched GaN-based laser diodes using focused ion beam etching, and analyzed¹¹ the results using the transfer matrix method. They concluded that the low reflectivities they obtained of 28%–38% were due to the etching. They showed in their analysis that the DBR stopband shifts to a shorter wavelength for a tilted sidewall. This result suggests that an increase in the semiconductor wall thickness might result in higher reflectivity. We have already confirmed, with regard to obtaining high reflectivity, that the optimal thickness of the semiconductor wall is greater than that based on the quarter wavelength design.¹² In our previous paper, we assumed a simple wafer structure consisting of three layers, where an active layer of $n_{\text{act}}=2.55$ was sandwiched between cladding layers of $n_{\text{clad}}=2.5$. We have also demonstrated highly reflective InGaN/GaN DBR mirrors based on an appropriate design.¹³ In our previous paper, we estimated the reflectivity from the threshold of the lasers and the estimated values ranged from 44% to 62% depending on the assumed internal loss.

In this letter, a deeply etched InGaN/GaN DBR mirror with tilted sidewalls is designed for the structure of a practical laser wafer utilizing the finite-difference time-domain (FDTD) method. The predicted optimal structure is different from the conventional quarter-wavelength design using a $\lambda/(4n)$ semiconductor and $\lambda/4$ air. If the sidewall of the grating is tilted, the reflectivity of the DBR mirrors decreases greatly. However, we can obtain high reflectivity even with tilted sidewalls, if the DBR structure is properly designed. We characterized the InGaN/GaN DBR mirrors that we fabricated based on the optimal design by the relation between the threshold pump intensity and the inverse of the cavity length, and obtained a high reflectivity of 62%.

The structure of the laser wafer is described in detail in Ref. 14. It consisted of a SiC substrate ($n_{\text{SiC}}=2.7$), an $n\text{-Al}_{0.08}\text{Ga}_{0.92}\text{N}$ lower cladding layer ($d=500$ nm, $n_{n\text{-AlGa}}=2.44$), an $n\text{-GaN}$ lower optical guiding layer ($d=100$ nm, $n_{\text{GaN}}=2.5$), an $\text{In}_{0.15}\text{Ga}_{0.85}\text{N}/\text{In}_{0.02}\text{Ga}_{0.98}\text{N}$ triple-quantum well active layer, a $p\text{-GaN}$ upper optical guiding layer ($d=100$ nm, $n_{\text{GaN}}=2.5$), a $p\text{-Al}_{0.2}\text{Ga}_{0.8}\text{N}$ upper cladding layer ($d=500$ nm, $n_{p\text{-AlGa}}=2.46$), and a $p\text{-GaN}$ contact layer ($d=50$ nm, $n_{\text{GaN}}=2.5$). In a simulation, the multiple-quantum well active layer was approximated as a single layer with a refractive index of 2.55 and a thickness of 17.5 nm, and the $p\text{-GaN}$ contact layer was ignored. The laser structure consisted of three pairs of deeply etched DBR mirrors [$5\lambda/(4n)$ semiconductor and $3\lambda/4$ air]. We adopted a higher-order DBR structure for two reasons. One was ease of fabrication, and the other was that a narrower air gap width means the air gaps cannot reach the active layer of the tilted sidewalls. The air gaps were etched as deep as $1.222\ \mu\text{m}$ into the SiC substrate.

Figure 1 shows the dependence of the calculated reflectivity on the sidewall angle of three DBR periods for a wavelength of $0.4\ \mu\text{m}$. We calculated the reflectivity using the FDTD method. In Fig. 1, the dashed and dotted lines, respec-

^{a)}Electronic mail: saito@nttbl.jp

^{b)}Present address: EIE, The Hong Kong Polytechnic University, Hong Kong.

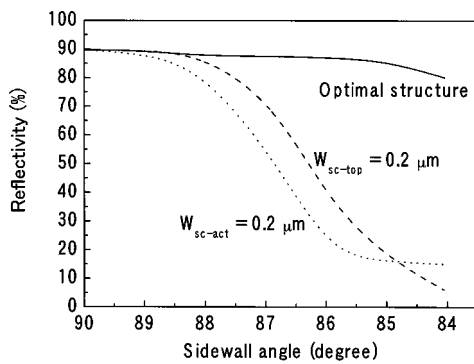


FIG. 1. Dependence of reflectivity on sidewall angle.

tively, denote the reflectivity when the top width of the semiconductor wall W_{sc-top} and the width at the active layer W_{sc-act} were both kept at $0.2 \mu\text{m}$. When we used a simple design consisting of a $5\lambda/(4n)$ ($0.2 \mu\text{m}$) semiconductor and $3\lambda/4$ ($0.3 \mu\text{m}$) air, the vertical sidewall tilt of only 4° reduced the reflectivity to less than 40% in both cases. However, a high reflectivity of more than 86% is predicted even for a sidewall angle of 86° , if the DBR structure is properly designed as represented by the solid line in Fig. 1. To achieve this, the semiconductor wall width at the active layer must be wider than $5\lambda/(4n)$ and the air gap width must be narrower than $3\lambda/4$. For example, when the sidewall angle is 84° , the optimum semiconductor width at the active layer is $0.266 \mu\text{m}$, which is far wider than the $0.2 \mu\text{m}$ derived from the conventional quarter-wavelength design. This result is qualitatively understandable when we take account of the interference of the reflected light from a parallel plate and a wedge. The optical path difference from the wedge is less than that from the parallel plate. In our previous report,¹² we calculated the reflectivity using a simple laser structure in which a $0.1 \mu\text{m}$ thick InGaN active layer was sandwiched between GaN layers. In such a weakly confined structure, the expected reflectivity for the same sidewall angle was only about 60%, even if we used an optimal design.

The laser wafer was grown on a (0001)-oriented *n*-type 6H-SiC substrate by metalorganic vapor phase epitaxy. The DBR structures were defined by electron-beam lithography and etched into the *n*-AlGaIn lower cladding layer by chlorine-based reactive ion etching (RIE). We have already confirmed that our RIE system causes little damage to either GaAs (Ref. 15) or GaN-based materials.¹⁶ A vertical sidewall is attainable for GaAs-based materials, however, it produces a sidewall angle of 86° in the deep etch of GaN-based materials. Taking this tilt angle into consideration, we designed the top width of the semiconductor as $0.16 \mu\text{m}$ to obtain highly reflective DBR structures. We varied the cavity length from $150 \mu\text{m}$ to $700 \mu\text{m}$. We designed the laser with a three-period DBR at each end of the cavity. Based on the FDTD calculation, three DBR periods provided sufficiently high reflectivity for laser oscillation. We also fabricated Fabry-Perot (FP) lasers on the same wafer for comparison.

A YVO_4/LBO laser emitting 10-ns-wide pulses at 355 nm with a repetition rate of 20 kHz was used for optical pumping at room temperature. A cylindrical lens focused the laser beam into a rectangular excitation spot on the sample surface to achieve uniform pumping. The emitted signal was

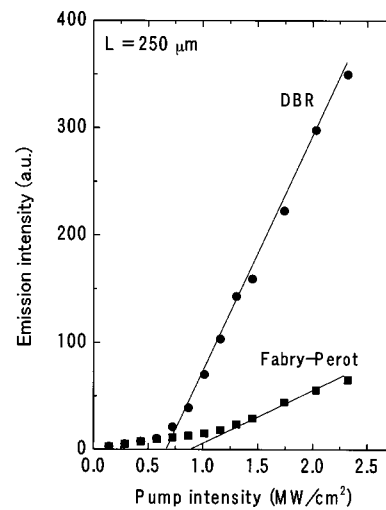


FIG. 2. Pump vs output emission characteristics.

collected from the normal to the sample surface in a 30 cm monochromator with a resolution of 0.26 nm. The light from the monochromator was detected with a charge-coupled-device array.

We operated both the DBR and FP lasers by optical pumping. Figure 2 shows the output emission intensity as a function of pumping intensity for DBR and FP lasers both with a cavity length of $250 \mu\text{m}$. Emission spectra are shown

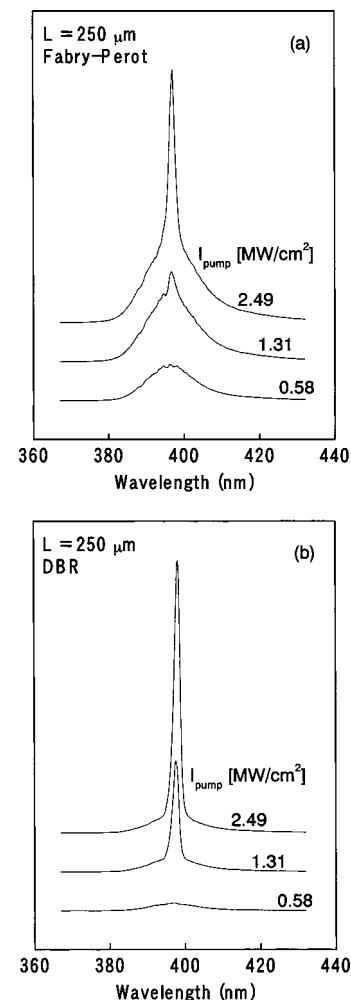


FIG. 3. Emission spectra for (a) FP and (b) DBR lasers.

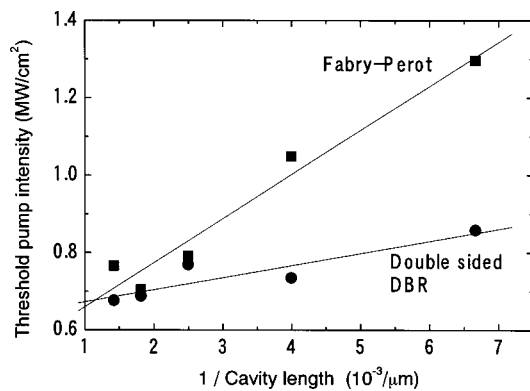


FIG. 4. Dependence of threshold pump intensity on inverse cavity length.

in Figs. 3(a) and 3(b) for FP and DBR lasers, respectively. The spontaneous emission intensity obtained at low pumping intensity was rather large because the emission output was detected from the normal to the laser substrate. As the pumping intensity increased, sharp and narrow emission spectra appeared. This emission structure became the dominant feature with further increases in pumping intensity. The threshold pumping intensity for laser oscillations was found to be ~ 0.65 MW/cm² for the DBR laser and ~ 0.9 MW/cm² for the FP laser.

The dependence of the threshold pump intensity on the inverse cavity length is shown in Fig. 4 for both DBR and FP lasers. The threshold pump intensity P_{th} is expressed by cavity length L and mirror reflectivity R as

$$P_{th} = \frac{C_1}{L} \ln(1/R) + C_2,$$

where C_1 and C_2 are constants. By comparing the slopes of the fitted lines in Fig. 4, the reflectivity of the DBR mirror is estimated to be 62% using a facet reflectivity value for the FP laser R_{FP} of 18%, which was also calculated with the FDTD method. This value is sufficiently large for the mirror reflectivity of InGaN/GaN lasers. However, this value is smaller than expected for optimally designed DBR mirrors. There are some possible reasons why this reflectivity is lower than the theoretical predictions. One is that the fabricated top width of the semiconductor wall was narrower ($W_{sc-top} = 0.13$ μm) than the optimal design ($W_{sc-top} = 0.16$ μm). Another is that the etched sidewall was not perfectly smooth. It should also be noted that the laser diodes were operating in a higher-order lateral mode because the lateral width of the focused pump laser beam was wider than 50 μm.

In conclusion, we designed and demonstrated highly reflective DBR mirrors for InGaN/GaN lasers with tilted sidewalls. The predicted optimal structure was different from the simple quarter-wavelength design using a $\lambda/(4n)$ semiconductor and $\lambda/4$ air. The calculation predicted that DBR mirrors with a sidewall tilt of 4° would reduce the reflectivity to less than 40%. However, if the DBR structure is properly designed, the decrease in the reflectivity compared with that of a perfectly vertical sidewall can be suppressed to only a few percent even with a sidewall tilt of 4°. We achieved InGaN/GaN DBR mirrors with a reflectivity as high as 62%. These design criteria will be useful for practical InGaN/GaN laser applications.

The authors express their gratitude to Dr. Yoshiro Hirayama, Dr. Takaaki Mukai, and Dr. Sunao Ishihara for their encouragement throughout the course of this work.

- ¹S. Nakamura, S. Pearton, and G. Fasol, *The Blue Laser Diode*, 2nd ed. (Springer, New York, 2000), p. 11.
- ²<http://www.blu-raydisc.info/>
- ³T. Baba, M. Hamasaki, N. Watanabe, P. Kaewplung, A. Matsutani, T. Mukaiharu, F. Koyama, and K. Iga, *J. Appl. Phys.* **35**, 1390 (1996).
- ⁴K. Shin, M. Tamura, A. Kasukawa, N. Serizawa, S. Kurihashi, S. Tamura, and S. Arai, *IEEE Photonics Technol. Lett.* **7**, 1119 (1995).
- ⁵S. Thomas and S. W. Pang, *J. Vac. Sci. Technol. B* **14**, 4119 (1996).
- ⁶Y. Yuan, T. Brock, P. Bhattacharya, C. Caneau, and R. Bhat, *IEEE Photonics Technol. Lett.* **9**, 881 (1997).
- ⁷S. Oku, S. Kondo, Y. Noguchi, T. Hirono, M. Nakao, and T. Tamamura, *Jpn. J. Appl. Phys., Part 1* **38**, 1256 (1998).
- ⁸E. Höfling, F. Schafer, and J. P. Reithmaier, *IEEE Photonics Technol. Lett.* **11**, 943 (1999).
- ⁹T. F. Krauss and R. M. De La Rue, *Appl. Phys. Lett.* **68**, 1613 (1996).
- ¹⁰C. Marinelli, L. J. Sargent, A. Wonfor, J. M. Rorison, R. V. Penty, I. H. White, P. J. Heard, G. Hasnain, and R. Schneider, *Electron. Lett.* **36**, 1706 (2000).
- ¹¹C. Marinelli, M. Bordovsky, L. J. Sargent, M. Gioannini, J. M. Rorison, R. V. Penty, I. H. White, P. J. Heard, M. Benyoucef, M. Kuball, G. Hasnain, M. Takeuchi, and R. P. Schneider, *Appl. Phys. Lett.* **79**, 4076 (2001).
- ¹²H. Wang, T. Tawara, M. Kumagai, T. Saitoh, and N. Kobayashi, *Jpn. J. Appl. Phys., Part 2* **41**, L682 (2002).
- ¹³H. Wang, M. Kumagai, T. Tawara, T. Nishida, T. Akasaka, N. Kobayashi, and T. Saitoh, *Appl. Phys. Lett.* **81**, 4703 (2002).
- ¹⁴T. Nishida, H. Saito, K. Kumakura, T. Makimoto, and N. Kobayashi, in *Proceedings of the International Workshop on Nitride Semiconductors 2000*, edited by the Institute of the Pure and Applied Physics (Nagoya Congress Center, Nagoya, Japan, 2000), p. 725.
- ¹⁵T. Saitoh, H. Gotoh, T. Sogawa, and H. Kanbe, *Mater. Res. Soc. Symp. Proc.* **442**, 63 (1997).
- ¹⁶N. Maeda, T. Saitoh, K. Tsubaki, T. Nishida, and N. Kobayashi, *Jpn. J. Appl. Phys., Part 2* **38**, L987 (1999).